REPORT NO.
UCB/SEMM-98/04

STRUCTURAL ENGINEERING
MECHANICS AND MATERIALS

TRIANGULAR FINITE ELEMENTS WITH ROTATIONAL DEGREES OF FREEDOM AND ENHANCED STRAIN MODES

BY

R. PILTNER and R.L. TAYLOR

APRIL 1998

DEPARTMENT OF CIVIL AND
ENVIRONMENTAL ENGINEERING
UNIVERSITY OF CALIFORNIA
BERKELEY, CALIFORNIA

TRIANGULAR FINITE ELEMENTS WITH ROTATIONAL DEGREES OF FREEDOM AND ENHANCED STRAIN MODES

R. PILTNER

Department of Engineering Mechanics, W317.2 Nebraska Hall,
University of Nebraska-Lincoln, Lincoln, NE 68588-0526, U.S.A.

R.L. TAYLOR

Department of Civil and Environmental Engineering, SEMM, University of California at Berkeley,
Berkeley, CA 94720, U.S.A.

Abstract

Three sets of enhanced strain functions are considered for the improvement of the three node triangular finite element with rotational degrees of freedom. In each case four enhanced strain terms are used. The four unknowns associated with the enhanced strain terms can be eliminated by static condensation so that nine degrees of freedom remain for the enhanced elements. Faster convergence in the energy norm is achieved. The enhanced elements are also able to deal with nearly incompressible plane strain problems considered provided all rotational degrees of freedom do not vanish in the boundary value problem.

KEYWORDS: Finite element method; enhanced strain method; plane stress/strain analysis

1. Introduction

The constant strain triangle (CST) with six degrees of freedom shows poor performance for problems with bending and for plane strain problems in the nearly incompressible limit. An improvement for bending problems was achieved by Allman by introducing rotational degrees of freedom at the element nodes [1,2]. However, in the nearly incompressible case the Allman element can still show locking problems (see examples in Section 5.6). Elements with rotational degrees of freedom also have been considered, for example, in references [1 - 14].

In recent years the concept of enhanced strains introduced by Simo and Rifai [15] has been used by several authors to improve the performance of low order finite elements (see references [15-21]). Simo and Rifai also found that the incompatible four node displacement element QM6 described in reference [22] can be viewed as an enhanced strain finite element with four enhanced strain terms. In this paper the concept of enhanced strains is used to develop improved triangular finite elements with rotational degrees of freedom. Three different possibilities of choosing the enhanced strain terms are considered. Several numerical examples are chosen to demonstrate the improvements due to the

enhanced strain terms.

2. Variational formulation

For our finite element approximation, we consider the following variational formulation [15]:

$$\Pi = \int_V \left[\frac{1}{2} \boldsymbol{\varepsilon}^T \mathbf{E} \boldsymbol{\varepsilon} - \mathbf{u}^T \bar{\mathbf{f}} \right] dV - \int_S \mathbf{u}^T \bar{\mathbf{T}} \, dS - \int_V \boldsymbol{\sigma}^T \boldsymbol{\varepsilon}^i \, dV \tag{1}$$

where the strains are decomposed into two parts according

$$\boldsymbol{\varepsilon} = \boldsymbol{\varepsilon}^c + \boldsymbol{\varepsilon}^i \tag{2}$$

The compatible displacement field $\mathbf{u}$ leads to the strains

$$\boldsymbol{\varepsilon}^c = \mathbf{D}\mathbf{u} = \mathbf{B}\mathbf{q} \tag{3}$$

where $\mathbf{B}$ is a strain matrix and $\mathbf{q}$ contains the nodal displacements and rotations. The enhanced strain field

$$\boldsymbol{\varepsilon}^i = \mathbf{B}^{enh} \boldsymbol{\lambda} \tag{4}$$

contains parameters $\boldsymbol{\lambda}$ which will be eliminated at the element level. Carrying out the variation in (1) we obtain

$$\int_V \delta(\mathbf{D}\mathbf{u})^T \left[\mathbf{E}(\mathbf{D}\mathbf{u} + \boldsymbol{\varepsilon}^i) \right] dV - \int_V \delta \mathbf{u}^T \bar{\mathbf{f}} \, dV - \int_S \delta \mathbf{u}^T \bar{\mathbf{T}} \, dS = 0 \tag{5}$$

$$\int_V (\delta \boldsymbol{\varepsilon}^i)^T \left[\mathbf{E}(\mathbf{D}\mathbf{u} + \boldsymbol{\varepsilon}^i) - \boldsymbol{\sigma} \right] dV = 0 \tag{6}$$

$$\int_V \delta \boldsymbol{\sigma}^T \boldsymbol{\varepsilon}^i \, dV = 0 \tag{7}$$

In the choice for the enhanced strains $\boldsymbol{\varepsilon}^i$ we are not completely free: In order to satisfy the patch test we have to impose the restriction on $\boldsymbol{\varepsilon}^i$ that constant stresses $\boldsymbol{\sigma}_c$ do no work on the enhanced strains [15]. This requirement can be expressed in the form

$$\int_V \delta \boldsymbol{\sigma}_c^T \boldsymbol{\varepsilon}^i \, dV = 0 \tag{8}$$

or equivalently as

$$\int_V \boldsymbol{\varepsilon}^i \, dV = \mathbf{0} \tag{9}$$

Equation (9) represents the minimum requirement in the enhanced strain method. In general we require in addition to (9) that the enhanced strains $\boldsymbol{\varepsilon}^i$ are orthogonal to reference stresses $\boldsymbol{\sigma}^*$ (see Table VII in reference [21]):

$$\int_V \delta\boldsymbol{\sigma}^{*T}\boldsymbol{\varepsilon}^i \, dV = \int_V \delta\boldsymbol{\varepsilon}^{iT}\boldsymbol{\sigma}^* \, dV = 0 \tag{10}$$

However, in the case of the triangular element with rotational degrees of freedom we do not have many higher order stress terms. There are only two linear terms in addition to the constant stress terms (see equation (22)). If we would require that the enhanced strains are also orthogonal to the linear stress terms *a priori*, we would not be able to calculate any parameters $\boldsymbol{\lambda}$ for the field $\boldsymbol{\varepsilon}^i$. Therefore, for the triangular enhanced strain element it will be sufficient to choose the reference stresses in the form

$$\boldsymbol{\sigma}^* = \begin{bmatrix} 1 & 0 & 0 \\ 0 & 1 & 0 \\ 0 & 0 & 1 \end{bmatrix} \boldsymbol{\beta} \tag{11}$$

and to set $\boldsymbol{\sigma} = \boldsymbol{\sigma}^*$. Since equation (7) is satisfied *a priori* with this choice of stresses, we cannot compute the stress parameters $\boldsymbol{\beta}$ from the variational formulation. Therefore the output stresses $\hat{\boldsymbol{\sigma}}$ will be computed from the element strains through

$$\hat{\boldsymbol{\sigma}} = \mathbf{E}(\mathbf{D}\mathbf{u} + \boldsymbol{\varepsilon}^i) \tag{12}$$

3. Finite element approximations

Using triangular area coordinates ξ_1, ξ_2, and ξ_3 the compatible displacement field for the triangular element with rotational degrees of freedom can be written as [1]:

$$u = u_1\xi_1 + u_2\xi_2 + u_3\xi_3 \tag{13}$$
$$+ \frac{1}{2}l_{12}\cos\gamma_{12}(\omega_2 - \omega_1)\xi_1\xi_2 + \frac{1}{2}l_{23}\cos\gamma_{23}(\omega_3 - \omega_2)\xi_2\xi_3 + \frac{1}{2}l_{31}\cos\gamma_{31}(\omega_1 - \omega_3)\xi_3\xi_1$$

$$v = v_1\xi_1 + v_2\xi_2 + v_3\xi_3 \tag{14}$$
$$+ \frac{1}{2}l_{12}\sin\gamma_{12}(\omega_2 - \omega_1)\xi_1\xi_2 + \frac{1}{2}l_{23}\sin\gamma_{23}(\omega_3 - \omega_2)\xi_2\xi_3 + \frac{1}{2}l_{31}\sin\gamma_{31}(\omega_1 - \omega_3)\xi_3\xi_1$$

Using the relationships

$$\cos\gamma_{ij} = n_x = \frac{y_j - y_i}{l_{ij}} \tag{15}$$

$$\sin\gamma_{ij} = n_y = -\frac{x_j - x_i}{l_{ij}} \tag{16}$$

$$y_{ji} = y_j - y_i\,, \qquad x_{ji} = x_j - x_i \tag{17}$$

$$l_{ij} = \sqrt{(x_j - x_i)^2 + (y_j - y_i)^2} \tag{18}$$

the displacement field can be rewritten in the form

$$u = u_1\xi_1 + u_2\xi_2 + u_3\xi_3 \tag{19}$$

$$+ \omega_1(-y_{21}\xi_1\xi_2 + y_{13}\xi_3\xi_1)/2 + \omega_2(y_{21}\xi_1\xi_2 - y_{32}\xi_2\xi_3)/2 + \omega_3(y_{32}\xi_2\xi_3 - y_{13}\xi_3\xi_1)/2$$

$$v = v_1\xi_1 + v_2\xi_2 + v_3\xi_3 \tag{20}$$

$$+ \omega_1(x_{21}\xi_1\xi_2 - x_{13}\xi_3\xi_1)/2 + \omega_2(-x_{21}\xi_1\xi_2 + x_{32}\xi_2\xi_3)/2 + \omega_3(-x_{32}\xi_2\xi_3 + x_{13}\xi_3\xi_1)/2$$

The compatible displacement field (19)-(20) leads to a strain field $\boldsymbol{\varepsilon}^c$ which can be written as

$$\boldsymbol{\varepsilon}^c = \hat{\mathbf{B}}\boldsymbol{\alpha} = \hat{\mathbf{B}}\mathbf{G}\mathbf{q} = \mathbf{B}\mathbf{q} \tag{21}$$

where

$$\hat{\mathbf{B}} = \begin{bmatrix} 1 & y & 0 & 0 & 0 \\ 0 & 0 & 1 & x & 0 \\ 0 & -x & 0 & -y & 1 \end{bmatrix} \tag{22}$$

and $\mathbf{q}^T = [\, u_1\ v_1\ \omega_1\ u_2\ v_2\ \omega_2\ u_3\ v_3\ \omega_3\,]$. The strain parameters $\boldsymbol{\alpha}$ are related to the nine nodal degrees of freedom through the matrix $\mathbf{G}$ which is given in the appendix of reference [1]. From equation (22) it is seen that the strain field $\boldsymbol{\varepsilon}^c$ contains only five linearly independent terms. Therefore the nine parameter Allman element has four eigenvalues equal to zero and at least one rotation parameter has to be prescribed in a finite element mesh in order to prevent the global system of equations from being singular.

4. Selection of enhanced strain modes

The choice of enhanced strain terms is not unique. Here we consider three different sets of enhanced strain terms.

4.1 First set of enhanced strain functions

In order to identify a possible set of enhanced strains in area coordinates we write a complete second order displacement field in the following form:

$$u = u_1\xi_1 + u_2\xi_2 + u_3\xi_3 \tag{23}$$

$$+ b_{12}y_{21}\xi_1\xi_2 + b_{23}y_{32}\xi_2\xi_3 + b_{31}y_{13}\xi_3\xi_1$$

$$+ a_{12}x_{21}\xi_1\xi_2 + a_{23}x_{32}\xi_2\xi_3 + a_{31}x_{13}\xi_3\xi_1$$

$$v = v_1\xi_1 + v_2\xi_2 + v_3\xi_3 \tag{24}$$

$$+ a_{12}y_{21}\xi_1\xi_2 + a_{23}y_{32}\xi_2\xi_3 + a_{31}y_{13}\xi_3\xi_1$$

$$- b_{12}x_{21}\xi_1\xi_2 - b_{23}x_{32}\xi_2\xi_3 - b_{31}x_{13}\xi_3\xi_1$$

The Allman displacement field is obtained if we set

$$b_{ij} = \frac{1}{2}(\omega_j - \omega_i)\,, \quad a_{ij} = 0 \tag{25}$$

However, the three quadratic displacement terms lead only to two deformation modes, because for the case that all element rotations ω_j are equal, the associated displacement contributions are zero. Therefore, the deformation mode associated with the coefficient

$$\lambda_1 = b_{12} = b_{23} = b_{31} \tag{26}$$

is not included in the Allman field and can be used to get the first enhanced strain term. If we choose

$$\lambda_2 = a_{12}, \quad \lambda_3 = a_{23}, \quad \lambda_4 = a_{31} \tag{27}$$

we get the remaining terms in the quadratic displacement expansion. Using the coupled incompatible displacement field

$$u = \lambda_1[\, y_{21}\xi_1\xi_2 + y_{32}\xi_2\xi_3 + y_{13}\xi_3\xi_1 \,] \tag{28}$$
$$+ \lambda_2 x_{21}\xi_1\xi_2 + \lambda_3 x_{32}\xi_2\xi_3 + \lambda_4 x_{13}\xi_3\xi_1$$

$$v = \lambda_1[\, - x_{21}\xi_1\xi_2 - x_{32}\xi_2\xi_3 - x_{13}\xi_3\xi_1 \,] \tag{29}$$
$$+ \lambda_2\, y_{21}\xi_1\xi_2 + \lambda_3\, y_{32}\xi_2\xi_3 + \lambda_4\, y_{13}\xi_3\xi_1$$

does not lead to strains which are orthogonal to constant stress terms. In order to make the resulting strains orthogonal to constant stress terms one can simply replace the area coordinates ξ_i by $\bar{\xi}_i = \xi_i - 1/3$. A similar approach for obtaining strains which are orthogonal to constant stresses was proposed in reference [23] where appropriate constant strains are added to an initial set of enhanced strains derived from an incompatible displacement field. The modification leads to the following enhanced strain matrix:

$$\mathbf{B}^{enh} = \begin{bmatrix} B_{11} & B_{12} & B_{13} & B_{14} \\ B_{21} & B_{22} & B_{23} & B_{24} \\ B_{31} & B_{32} & B_{33} & B_{34} \end{bmatrix} \tag{30}$$

where

$$B_{11} = \frac{1}{2A}(a_y y_{23} + b_y y_{31} + c_y y_{12}) \quad , \quad B_{21} = \frac{1}{2A}(a_x x_{23} + b_x x_{31} + c_x x_{12})$$

$$B_{31} = \frac{1}{2A}(a_y x_{32} + b_y x_{13} + c_y x_{21} + a_x y_{32} + b_x y_{13} + c_x y_{21})$$

$$B_{12} = -\frac{c_y x_{21}}{2A} \quad , \quad B_{22} = \frac{c_x y_{21}}{2A} \quad , \quad B_{32} = \frac{c_x x_{21} - c_y y_{21}}{2A} \tag{31}$$

$$B_{13} = -\frac{a_y x_{32}}{2A} \quad , \quad B_{23} = \frac{a_x y_{32}}{2A} \quad , \quad B_{33} = \frac{a_x x_{32} - a_y y_{32}}{2A}$$

$$B_{14} = -\frac{b_y x_{13}}{2A} \quad , \quad B_{24} = \frac{b_x y_{13}}{2A} \quad , \quad B_{34} = \frac{b_x x_{13} - b_y y_{13}}{2A}$$

and

$$
\begin{aligned}
&2A = x_{21}y_{31} - x_{31}y_{21} \\
&a_x = x_{21}(\xi_2 - \frac{1}{3}) + x_{13}(\xi_3 - \frac{1}{3}) \quad , \quad a_y = y_{21}(\xi_2 - \frac{1}{3}) + y_{13}(\xi_3 - \frac{1}{3}) \\
&b_x = x_{21}(\xi_1 - \frac{1}{3}) + x_{32}(\xi_3 - \frac{1}{3}) \quad , \quad b_y = y_{21}(\xi_1 - \frac{1}{3}) + y_{32}(\xi_3 - \frac{1}{3}) \\
&c_x = x_{32}(\xi_2 - \frac{1}{3}) + x_{13}(\xi_1 - \frac{1}{3}) \quad , \quad c_y = y_{32}(\xi_2 - \frac{1}{3}) + y_{13}(\xi_1 - \frac{1}{3})
\end{aligned}
\tag{32}
$$

The resulting element, denoted TE4, is frame invariant. In the numerical examples frame invariance is verified by describing each problem in a series of different rotated frames.

4.2 Second set of enhanced strain functions

Using the local cartesian coordinates $\bar{x}$, $\bar{y}$ which are related to the global coordinates x, y and the area coordinates ξ_1, ξ_2, and ξ_3 through

$$
\begin{aligned}
&\bar{x} = x - x_0 = (\xi_1 - \frac{1}{3})x_1 + (\xi_2 - \frac{1}{3})x_2 + (\xi_3 - \frac{1}{3})x_3 \\
&\bar{y} = y - y_0 = (\xi_1 - \frac{1}{3})y_1 + (\xi_2 - \frac{1}{3})y_2 + (\xi_3 - \frac{1}{3})y_3
\end{aligned}
\tag{33}
$$

we can choose the following enhanced strain matrix:

$$
\mathbf{B}^{enh} = \begin{bmatrix} \bar{x} & 0 & 0 & 0 \\ 0 & \bar{y} & 0 & 0 \\ 0 & 0 & \bar{x} & \bar{y} \end{bmatrix} \tag{34}
$$

The resulting element, denoted TE4_1, gives improved results. However, the element is not frame invariant. In order to make the results at least independent of the finite element user's input data one can choose the local cartesian coordinates depending on the geometric features of the triangle: One could choose the local $\bar{x}$ axis to be parallel to the largest edge of the triangle. If the element has two equal edges the $\bar{x}$-axis is chosen to be parallel to the third edge. If all edges are equal it does not matter which one is chosen for the alignment of the local coordinates. In the search for optimal enhanced strain terms several other combinations of $\bar{x}$ and $\bar{y}$ terms in the $\mathbf{B}^{enh}$-matrix have been tested in numerical examples. Most of the other choices considered gave worse results. An exception was a set of enhanced strain terms presented in the next sub-section.

4.3 Third set of enhanced strain functions

The following choice of enhanced strains leads to a frame invariant element:

$$\mathbf{B}^{enh} = \begin{bmatrix} \bar{x} & 0 & \bar{y} & 0 \\ 0 & \bar{y} & 0 & \bar{x} \\ -\bar{y} & -\bar{x} & \bar{x} & \bar{y} \end{bmatrix} \tag{35}$$

The element will be denoted TE4_2.

5. Numerical examples

Several problems have been chosen in order to test the performance of the three-node elements with four enhanced strain modes. The results are compared to analytical solutions and to results obtained from the constant strain triangle (CST) and the original Allman element. For the element TE4 the enhanced strain matrix (30) is used, whereas for element TE4_1 the enhanced strains (34) are used, and element TE4_2 employs the enhanced strains (35). All elements we compare are implemented in the finite element program FEAP (e.g. see Chapter 15 of reference [24]).

5.1 Patch test

For the patch test a rectangular domain of length a=0.24 and width b=0.12 is modeled with ten triangular elements and plane stress conditions are assumed (Figure 1). The material parameters are $E = 10x10^6$, $\nu = 0.25$ and the thickness is $t = 0.001$. As in the test of MacNeal/Harder [25] the boundary conditions for the boundary nodes are calculated from the displacement field

$$\begin{aligned} u &= 10^{-3}(x + y/2) \\ v &= 10^{-3}(y + x/2) \end{aligned} \tag{36}$$

which satisfies the Navier-equations. The considered enhanced elements give in this test the exact values for the stresses and strains which are given by $\varepsilon_{xx} = \varepsilon_{yy} = \gamma_{xy} = 10^{-3}$, $\sigma_{xx} = \sigma_{yy} = 1333$, $\tau_{xy} = 400$.

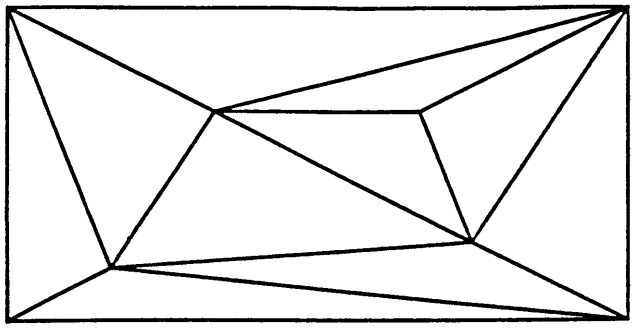

Figure 1: Finite element mesh for the patch test

5.2 Curved beam

The curved beam shown in Figure 2 is fixed at the upper end and bent by a unit force applied at the lower end in radial direction. The material parameters are E = 1000 and $\nu = 0$. The exact solution is taken from Timoshenko/Goodier [26]. The enhanced triangular elements show improved results compared to the Allman element (Table 1). For the considered mesh, the displacement obtained with the CST element is still far away from the exact solution.

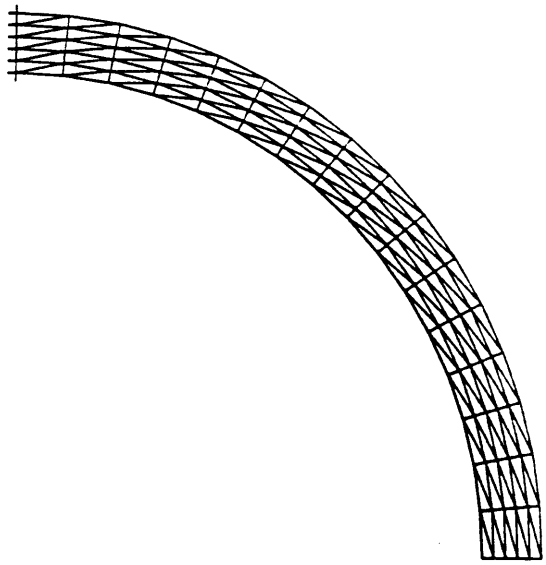

Figure 2: Finite element mesh for curved beam problem

Table 1: Results for the curved beam problem shown in Figure 2 (assuming plane stress conditions) E=1000, ν=0,

tip displacement					
exact	CST	Allman	TE4	TE4_1	TE4_2
5.800	2.729	5.158	5.622	5.714	5.733

5.3 Beam bending: coarse mesh test

A beam modeled with twenty elements is subjected to two load cases (Figure 3). Warping at the left end of the beam is possible. Plane stress conditions are assumed in the model. The results of five different elements for the maximum displacement at point A and the normal stress σ_{xx} at point B are given in Table 2. The stress at point B was calculated at an element Gauss-point. The three Gauss-points of the triangular element were chosen as the midside points of the the three element edges. The material parameters are E = 1500 and ν = 0.25. Element TE4_2 appears to be a very flexible element giving displacements which are larger than the exact ones.

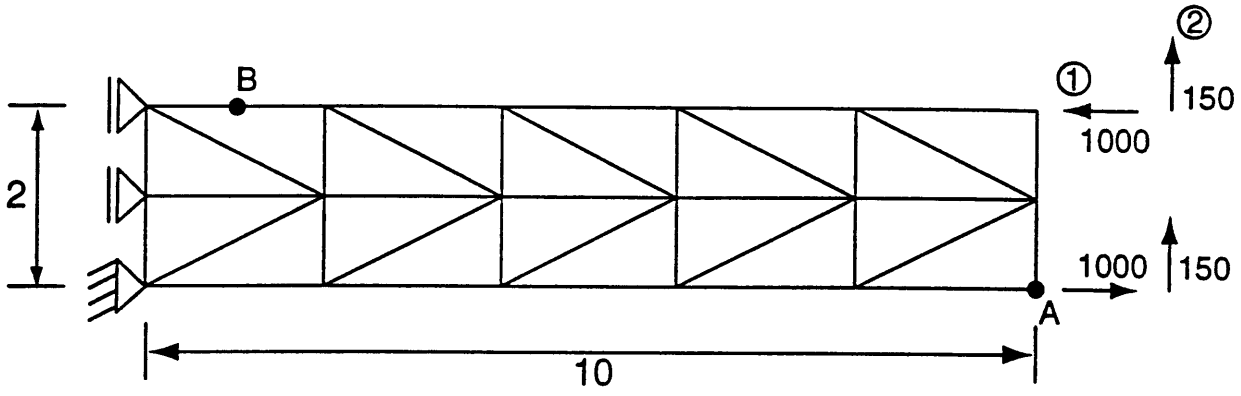

Figure 3: Finite element mesh for cantilever beam problem

Table 2: Comparison of plane stress solutions obtained with triangular elements for cantilever beam problems.

	Case 1		Case 2	
element	v_A	σ_{xxB}	v_A	σ_{xxB}
CST	37.14	-1165	39.49	-1590
Allman	86.54	-2676	88.06	-3624
TE4	91.64	-2908	92.95	-3927
TE4_1	96.26	-2936	97.92	-3947
TE4_2	102.0	-2743	102.4	-3676
exact	100	-3000	102.6	-4050

5.4 Cook's membrane problem

The plane stress structure shown in Figure 4 was suggested by Cook [27] as a test for membrane elements in skewed meshes. The material parameters are E = 1 and ν = 1/3. The shear load is distributed uniformly along the right edge. Table 3 gives the displacements, stresses and energy results for different meshes. For a comparison the results for the quadrilateral QM6 element are also included for a 16x16 mesh. Considering both stress and displacement results, element TE4 appears to give the best overall performance in this example.

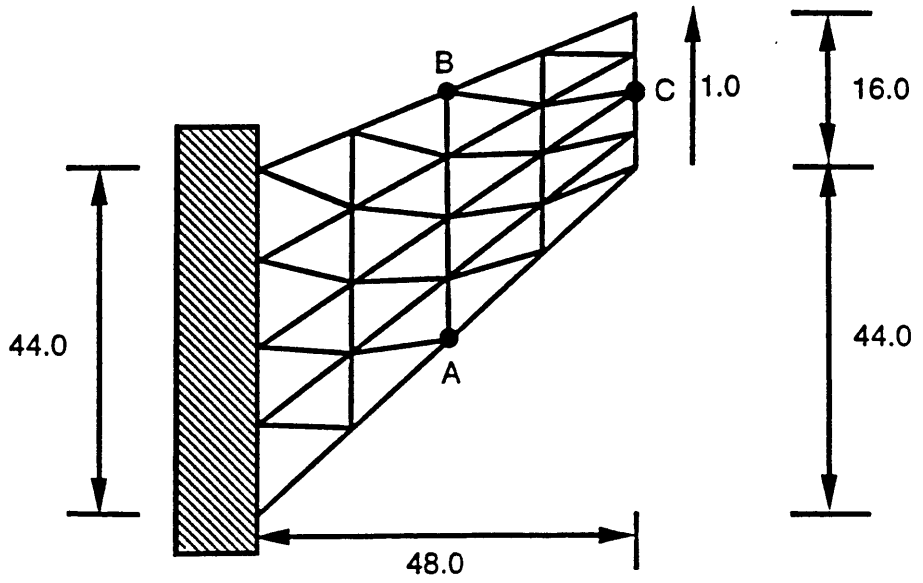

Figure 4: Cook's membrane problem: plane stress structure with unit load uniformly distributed along right edge (E = 1, ν = 1/3).

Table 3: Results for the problem shown in Figure 4.

displacement v at C			
element	N=2	N=4	N=16
CST	11.99	18.28	23.41
Allman	19.67	22.41	23.81
TE4	20.27	22.49	23.81
TE4_1	20.74	22.64	23.82
TE4_2	21.14	22.64	23.83
QM6			23.88

maximum stress at A			
element	N=2	N=4	N=16
CST	0.0760	0.1498	0.2217
Allman	0.1523	0.2047	0.2324
TE4	0.1640	0.2085	0.2336
TE4_1	0.1587	0.2061	0.2326
TE4_2	0.1491	0.1973	0.2299
QM6			0.2364

energy			
element	N=2	N=4	N=16
CST	11.99	18.27	23.42
Allman	19.68	22.44	23.86
TE4	20.53	22.71	23.89
TE4_1	21.03	22.85	23.90
TE4_2	21.77	23.12	23.93
QM6			23.93

5.5 Cantilever beam under a tip load: convergence study

In this example the left end of the beam is fixed and at the right end a parabolic shear distribution is applied (Figure 5). The material parameters of the plane stress structure are $E = 3.0*10^7$ and $\nu = 0.25$. The results are shown in Table 4.

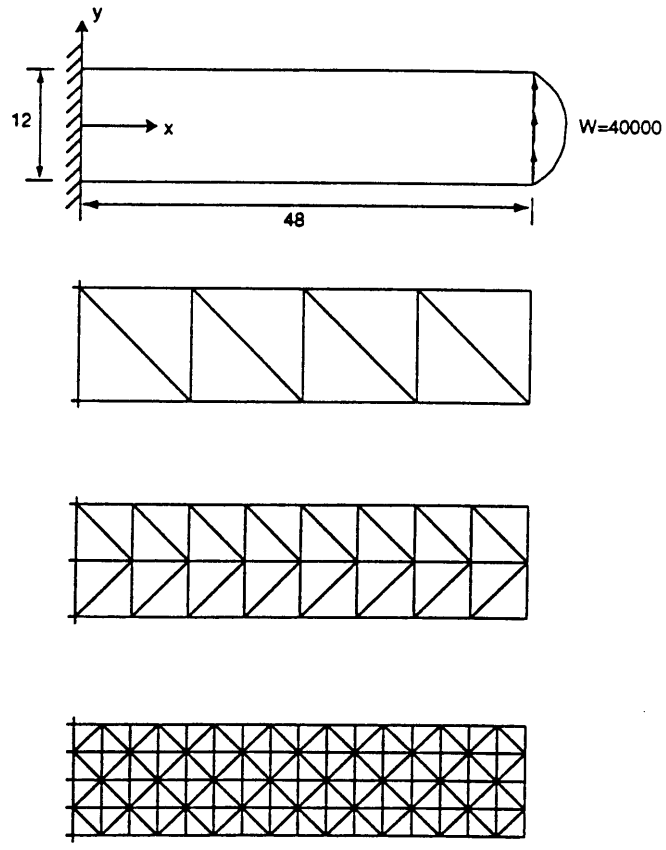

Figure 5: Cantilever beam and three meshes

Table 4: Results for the problem shown in Figure 5 (Allman's beam example).

displacement v at x = 48, y = 0					
mesh	CST	Allman	TE4	TE4_1	TE4_2
1 x 4	0.0907	0.2696	0.3037	0.3348	0.4033
2 x 8	0.1984	0.3260	0.3382	0.3471	0.3652
4 x 16	0.3056	0.3472	0.3506	0.3530	0.3567
8 x 32	0.3421	0.3539	0.3548	0.3554	0.3563
16 x 64	0.3531	0.3560	0.3562	0.3564	0.3566
exact	0.3566				

Energy / 10^3					
mesh	CST	Allman	TE4	TE4_1	TE4_2
1 x 4	3.63	10.78	12.15	13.39	16.11
2 x 8	7.94	13.05	13.54	13.90	14.63
4 x 16	12.23	13.90	14.04	14.14	14.30
8 x 32	13.69	14.17	14.21	14.24	14.29
16 x 64	14.14	14.26	14.27	14.28	14.30
exact	14.28				

5.6 Plane strain problem in the nearly incompressible case

In order to test the behavior of the enhanced triangular elements we look at a plane strain system with one very coarse and two fine mesh discretizations (Figures 6 and 7). The numerical results are shown in Tables 5 and 6. The material parameters are E = 1500 and ν = 0.49/0.499/0.4999/0.49999. For the coarse mesh the CST and the Allman element lock in the nearly incompressible case. It is known that for special mesh patterns locking can be avoided for the CST element as it is the case for mesh 1 in Figure 7. (Remark: In reference [28] Hughes and Taylor found a superior performance of linear triangular bending elements in cross-diagonal mesh patterns when compared to other mesh patterns.) In general however, the CST and the Allman element will lock also for a fine discretization as, for example, for mesh 2 shown in Figure 7. The enhanced triangular elements do not lock except for the case when due to symmetry conditions in the problem all rotational degrees of freedom vanish a priori. For a problem with vanishing rotations one can add constant pressure to the triangular enhanced element.

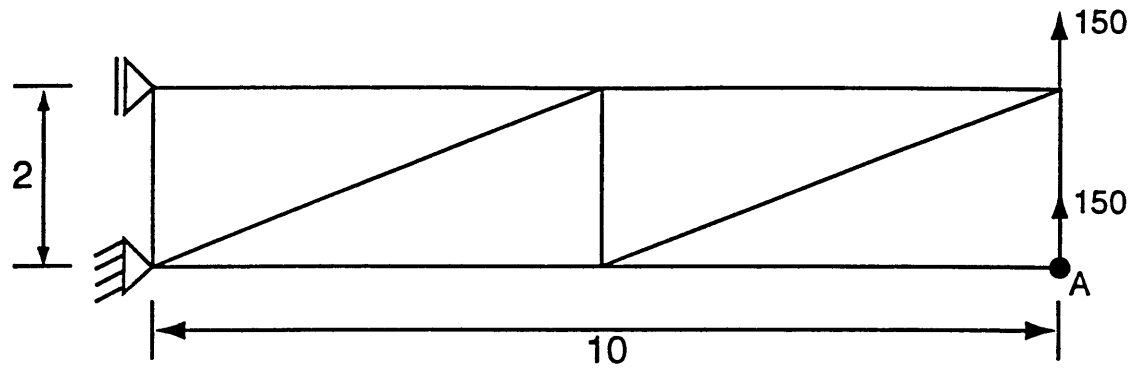

Figure 6: Plane strain structure with resultant shear force 2P = 300

Table 5: Results for the beam problem shown in Figure 6 assuming plane strain conditions and different values of ν in the nearly incompressible range.

displacement v at A					
ν	CST	Allman	TE4	TE4_1	TE4_2
0.49	12.27	22.25	51.25	41.25	75.27
0.499	12.13	13.43	50.78	39.94	74.64
0.4999	12.11	12.24	50.73	39.81	74.58
0.49999	12.11	12.12	50.73	39.80	74.57
exact	78.375				

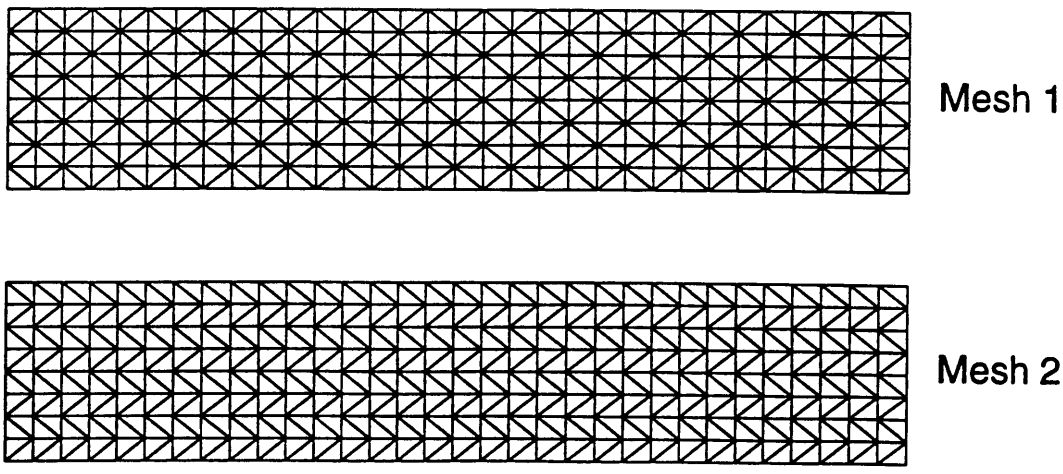

Figure 7: Two fine meshes for the beam problem shown in Figure 6.

Table 6: displacement results for the meshes shown in Figure 7.

displacement v at A (case: v=0.49999)					
mesh	CST	Allman	TE4	TE4_1	TE4_2
1	76.23	76.47	78.16	77.79	78.50
2	3.73	9.21	77.86	77.57	78.37
exact	78.375				

6 Concluding remarks

Three different enhanced strain fields have been used to obtain improved triangular elements with three rotational degrees of freedom. Each set of enhanced strains involves four enhanced strain parameters which can be eliminated at the element level. Element TE4_2 appears to be the most flexible element. The disadvantage of element TE4_1 is that it is not frame invariant, and making the element independent of the finite element user by pre-defining preferred local coordinate orientations is not completely satisfactory although improved results can be obtained with element TE1_1. Element TE4 shows an overall good behavior both for displacement and stress results. The enhanced strains for element TE4 and TE4_2 not only satisfy the minimum requirement of being orthogonal to constant stress terms but also yield frame invariant elements. There might be other invariant sets of enhanced strains which possibly yield even better results. Since there is no unique way to choose the enhanced strain terms, it would be interesting for future research whether some additional "quality" criteria and conditions in addition to equation (9) can be defined in order to construct an optimal set of enhanced strains.

REFERENCES

[1] D. J. Allman, "A compatible triangular element including vertex rotations for plane elasticity analysis", Computers & Structures, 19 (2), 1 - 8, (1984).

[2] D. J. Allman, 'Evaluation of the Constant Strain Triangle with Drilling Rotations', International Journal for Numerical Methods in Engineering, 26(12), 2645-2655, (1988).

[3] D. J. Allman, 'A Quadrilateral Finite Element Including Vertex Rotations for Plane Elasticity Analysis', International Journal for Numerical Methods in Engineering, 26(3), 717-730, (1988).

[4] D. J. Allman, 'Variational Validation of a Membrane Finite Element with Drilling Rotations', Communications in Numerical Methods in Engineering, 9(4), 345-351, (1993).

[5] P.G. Bergan and C.A. Felippa, "A triangular membrane element with rotational degrees of freedom", Comp. Meth. Appl. Mech. Eng., 50, 25 - 69, (1985)

[6] R. D. Cook, "On the Allman triangle and a related quadrilateral element", Computers & Structures, 22 (6), 1065 - 1067, (1986).

[7] R. D. Cook, "A plane hybrid element with rotational D.O.F. and adjustable stiffness", International Journal for Numerical Methods in Engineering, 24, 1499 - 1508, (1987).

[8] R. D. Cook, 'Modified Formulations for Nine-DOF Plane Triangles that Include Vertex Rotations', International Journal for Numerical Methods in Engineering, 31(5), 825-835, (1991).

[9] Hughes, T.J.R., Masud, A. and Harari, I., Numerical assessment of some membrane elements with drilling degrees of freedom, Computers & Structures, 55 (2), 297-314, (1995).

[10] T. J. R. Hughes, A. Masud, and I. Harari, 'Dynamic Analysis and Drilling Degrees of Freedom', International Journal for Numerical Methods in Engineering, 38(19), 3193-3210, (1995).

[11] A. Ibrahimbegovic, R. L. Taylor, and E. L. Wilson, 'A Robust Quadrilateral Membrane Finite Element with Drilling Degrees of Freedom', International Journal for Numerical Methods in Engineering, 30(3), 445-457, (1990).

[12] T. P. Pawlak, S. M. Yunus, and R. D. Cook, 'Solid Elements with Rotational Degrees of Freedom: Part II--Tetrahedron Elements', International Journal for Numerical Methods in Engineering, 31(3), 593-610, (1991).

[13] S. M. Yunus, T. P. Pawlak, and R. D. Cook, 'Solid Elements with Rotational Degrees of Freedom: Part 1--Hexahedron Elements', International Journal for Numerical Methods in Engineering, 31(3), 573-592, (1991).

[14] S. M. Yunus, S. Saigal, and R. D. Cook, 'On Improved Hybrid Finite Elements with Rotational Degrees of Freedom', International Journal for Numerical Methods in Engineering, 28(4), 785-800, (1989).

[15] J.C. Simo and M.S. Rifai, "A class of mixed assumed strain methods and the method of incompatible modes", Int. J. Numer. Meth. Eng., 29, 1595 - 1638, (1990).

[16] J.C. Simo and F. Armero, "Geometrically non-linear enhanced strain mixed methods and the method of incompatible modes", Int. J. Numer. Meth. Eng., 33, 1413 - 1449, (1992).

[17] J.C. Simo, F. Armero and R. L. Taylor, "Improved versions of assumed enhanced strain tri-linear elements for 3D finite deformation problems", Comput. Methods Appl. Mech. Engrg. 110, 359 - 386, (1993).

[18] U. Andelfinger and E. Ramm, "EAS-elements for two-dimensional, three-dimensional, plate and shell structures and their equivalence to HR-elements", Int. J. Numer. Meth. Eng., 36, 1311 - 1337, (1993).

[19] C. Freischläger and K. Schweizerhof, "On a systematic development of trilinear three-dimensional solid elements based on Simo's enhanced strain formulation", International Journal of Solids and Structures, 33, 2993-3017, (1996).

[20] P. Wriggers and J. Korelc, "On enhanced strain methods for small and finite deformations of solids", Computational Mechanics, 18, 413 - 428, (1996).

[21] R. Piltner and R.L. Taylor, "A quadrilateral finite element with two enhanced strain modes", Int. J. Numer. Meth. Eng., 38, 1783 - 1808, (1995).

[22] R.L. Taylor, P.J. Beresford and E.L. Wilson, "A non-conforming element for stress analysis", Int. J. Numer. Meth. Eng., 10, 1211 - 1219, (1976).

[23] A. Ibrahimbegovic and E.L. Wilson, "A modified method of incompatible modes", Communications in Applied Numerical Methods, 7, 187 - 194, (1991).

[24] O.C. Zienkiewics / R.L. Taylor, "The Finite Element Method", Vol. 1, McGraw Hill, London, New York, 1989.

[25] R.H. MacNeal and R.L. Harder, "A proposed standard set of problems to test finite element accuracy", Finite Elements in Analysis and Design, 1, 2 - 20, (1985).

[26] S.P. Timoshenko and J.N. Goodier, "Theory of Elasticity", McGraw Hill, New York, 1970.

[27] R.D. Cook/ D.S. Malkus/ M.E. Plesha, "Concepts and Applications of Finite Element Analysis", John Wiley & Sons, New York 1989

[28] T.J.R. Hughes and R.L. Taylor, "The linear triangular bending element", pp. 127 - 142, in: The Mathematics of Finite Elements and Applications IV (MAFELAP 1981), J.R Whiteman (Ed.), Academic Press, London, New York, 1982.